Quantum Electronics **39** (6) 531 – 536 (2009)

INTERACTION OF LASER RADIATION WITH MATTER. LASER PLASMA

PACS numbers: 52.50.Jm; 52.38.Mf; 52.57.Fg
DOI: 10.1070/QE2009v039n06ABEH014125

Smoothing of ablation pressure nonuniformities in the laser-plasma corona during heating of laser fusion targets

M.A. Zhurovich, O.A. Zhitkova, I.G. Lebo, Yu.A. Mikhailov, G.V. Sklizkov, A.N. Starodub, V.F. Tishkin

***Abstract*. A method for smoothing ablation pressure nonuniformities during heating of laser fusion targets is described which utilises an extra laser pulse preceding the main pulse. Theoretical and experimental data are presented on heating of thin (3 – 10 μm) foils (simulating the target shell) by a spatially nonuniform laser beam. In the experiments, the laser pulse width at half maximum was 2 ns and the pulse energy was 2 – 30 J, which ensured a power density on the target surface from 10^{13} to 10^{14} W cm^{-2}. The experimental data are analysed using two-dimensional numerical simulations. The experimental and simulation results demonstrate that this approach is sufficiently effective. The optimal laser prepulse parameters are determined.**

Keywords: *laser fusion plasma, ablation pressure in the plasma corona, irradiance smoothing*.

1. Introduction

To achieve high energy gains in reactor-scale laser fusion systems, the target fuel must be compressed to densities four to five orders of magnitude above its initial density. To this end, use is made of multibeam laser systems, which must ensure the maximum possible uniformity of the laser irradiance on the fusion target and, hence, uniform heating of its shell. There are, however, a number of obstacles to producing a uniform laser intensity distribution on the target surface, the most important of which are the interference of highly coherent overlapping beams and the nonuniform intensity profile of each beam due to various defects in the laser channels. This leads to nonuniform heating of the target shell, thereby disturbing the ablation pressure front in the laser-plasma corona and giving rise to hydrodynamic instabilities, which entail a dramatic asymmetry in target compression and may cause the target to disintegrate [1, 2]. Therefore, the ability to reduce (smooth down) ablation pressure nonuniformities is critical for creating energetically viable laser fusion facilities.

Bokov et al. [3] proposed using a laser prepulse to generate a high-temperature dense plasma capable of reducing nonuniformities in the heating of a spherical target, and Ilyasov et al. [4] reported preliminary results of experimental and theoretical studies on this problem. Gamaly et al. [5] and Lebo et al. [6] used two-dimensional (2D) numerical simulations to assess the effectiveness of this approach when the prepulse and main (heating) pulse have the same wavelength ($\lambda \sim 1$ μm) [5] and when the main pulse has a shorter wavelength than does the prepulse (the third and fundamental iodine laser harmonics, respectively) [6]. The point is that the target compression efficiency increases with decreasing heating pulse wavelength. Therefore, the main pulse must be generated at high harmonics. This, however, would give rise to energy losses and may produce additional target heating nonuniformities. As shown by Lebo et al. [6], the effectiveness of irradiance smoothing with the use of the corona produced by a prepulse depends little on the heating pulse wavelength. In view of this, we believe that the prepulse approach is of interest for reactor-scale laser systems, where the energy efficiency may be of key importance.

Ivanov et al. [7] reported experimental results, obtained on the Pico facility (Nd laser, P.N. Lebedev Physics Institute (LPI), Russian Academy of Sciences), on anomalous burn-through of thin aluminium foils. The experiments were computer-simulated using the NUTCY 2D Euler code [8]. The experimental results showed that a small part of the laser radiation penetrated through foils more than 3 – 5 μm in thickness, whereas simulations for a smooth Gaussian beam profile suggested that the laser pulse was too short for through holes to form in the foil. The reason for the anomalous burn-through of the foils is that the laser beam front is not smooth but consists of speckles, which are considerably smaller in size than the focal spot. This gives rise to a 'micropiercing' effect. Ivanov et al. [7] discussed the possibility of suppressing this detrimental effect by a laser prepulse.

Experiments on the Perun facility (iodine laser, Czech Republic) [9, 10] have demonstrated that a laser prepulse is an effective means of smoothing ablation pressure nonuniformities. A laser beam was split into three beams, two of which were frequency-tripled (blue), and one was frequency-doubled (red) or left unconverted at the fundamental frequency (infrared). The blue beams were delayed by time Δt relative to the first beam (the time delay was varied)

M.A. Zhurovich, Yu.A. Mikhailov, G.V. Sklizkov, A.N. Starodub
P.N. Lebedev Physics Institute, Russian Academy of Sciences, Leninsky prosp. 53, 119991 Moscow, Russia; e-mail: mikh@sci.lebedev.ru;
O.A. Zhitkova, I.G. Lebo Moscow State Institute of Radio-Engineering, Electronics and Automation (Technical University), prosp. Vernadskogo 78, 119454 Moscow, Russia;
V.F. Tishkin Institute of Mathematical Modelling, Russian Academy of Sciences, Miusskaya pl. 4a, 125047 Moscow, Russia

Received 26 March 2009
Kvantovaya Elektronika **39** (6) 531 – 536 (2009)
Translated by O.M. Tsarev

and were focused to small spots of higher intensity in comparison with the first beam. The targets used were 7-μm-thick aluminium foils. The experiments indicated partial 'piercing' of the foils by the blue beams. The highest smoothing efficiency was achieved at a delay time $\Delta t = 0.5$ ns, in perfect agreement with the results of 2D numerical simulations using the Atlant-C code [11].

Lebo et al. [12] considered conversion of a smoothing laser pulse to X-rays. They proposed surrounding the target with a layer of low-density porous material that would support a heavy-metal (copper or gold) converter shell. Laser pulse to X-ray conversion is accompanied by significant energy losses but makes it possible to suppress the small-scale disturbance of the laser flux. In addition, it was proposed to expose the target to two pulses: a prepulse and main pulse. The converter must then be thin enough to vaporise after the prepulse but to ensure generation of an X-ray prepulse. As shown by 2D numerical simulations, the generation of high ($n \geqslant 20$) plasma density harmonics due to the small-scale disturbance of the laser flux can be effectively suppressed using such an X-ray prepulse. To compensate the influence of large-scale ($n \sim 2-4$) heating nonuniformities, related to the laser facility design, on the compression of the target, it was proposed to use a special profile of the target.

Note that Bokov et al. [3] examined the feasibility of using a low-density coating on the target in order to reduce the effect of laser heating nonuniformities. After the advent of techniques for the fabrication of porous materials with a tailored structure, this area of research has received considerable theoretical and experimental attention (see, e.g. [13–17]), but this issue is beyond the scope of this report.

In this paper, we present a detailed analysis of experimental data on the smoothing of ablation pressure nonuniformities in the laser-plasma corona on the Pico facility at the Laboratory of Laser Plasma, LPI. We examine the smoothing effect of a prepulse having the same wavelength as the main pulse, at various prepulse energies and main-pulse delays relative to the prepulse. In addition, we present theoretical interpretation of the experimental results.

2. Formulation of the problem

When absorbed in the critical plasma density region produced by a prepulse, a nonuniform main laser pulse gives rise to nonuniform heating of this region. The deposited energy is transferred to the bulk of the dense target material by heat flow, and transverse heat conduction reduces the speckle disturbances of the temperature and pressure. Note that, in theoretical studies, one has to solve not only non-1D heat equations but also nonlinear hydrodynamic and radiative transfer equations, which cannot be done without numerical modelling techniques.

Our experimental studies were concerned with the effect of the spatiotemporal prepulse structure on the fraction of energy transmitted through the foil with the aim of optimising the relationship between the main pulse and prepulse energies and the main-pulse delay in order to reduce ablation pressure nonuniformities.

Numerical simulations were performed with the NUTCY 2D code in Eulerian cylindrical coordinates. The Euler code was used because, in our experiments, we measured the fraction of energy transmitted through the plasma layer as a result of the formation of a through hole in the dense layer. Modelling such experiments in Lagrangian coordinates is hindered by the strong distortion of the mesh cells in response to foil burn-through.* The simulation parameters paralleled the experimental conditions.

3. Experimental setup

The interaction between laser radiation and thin foils was studied on the Pico facility, built around a single-channel Nd^{3+}-doped GLS-1 glass laser. The laser beam was focused in a diagnostic vacuum chamber, which contained aluminium foil samples simulating the fusion target shell.

The laser was operated in a Q-switching regime, with a pulse duration of 30 ns at the oscillator output, pulse energy of 0.1 J and bandwidth $\delta\lambda \approx 30$ Å. The pulse was amplified in several stages, with the formation of a narrow pulse after the first stage using a Pockels cell. At the laser output, the pulse width at half maximum was ~ 2 ns and the pulse energy 2–30 J. The beam was focused in the diagnostic chamber by a lens with a focal length $f = 10$ cm, leading to a power density on the target surface from 10^{13} to 10^{14} W cm^{-2}. The energy contrast of the beam was 10^4 to 10^5, and the beam divergence was $2\alpha = (5-8) \times 10^{-4}$ rad.

The prepulse was produced by splitting the parent pulse after it had passed the Pockels cell, using mirrors with different transmittances. The number of prepulse amplification stages and the optical path of the prepulse can be varied, which makes it possible to obtain energies in the range 10^{-3} to 10^{-1} of the main pulse energy and delay times from 0.5 to 5 ns. The spatial structure of the prepulse was smoothed by a special phase plate.

The energy parameters of the process (the energies of the main pulse, prepulse and radiation transmitted through the foil and scattered in different directions) were determined using a calorimetric system which incorporated VChD-2, VChD-3, VChD-5, VKDS and KDV calorimeters, designed at the Special Design Bureau, LPI. The system enabled energy measurements in the range 10^{-5} to 10^2 J with an uncertainty of 6 % – %. The temporal structures of the incident and transmitted beams were recorded by coaxial photoelectric cells with a temporal resolution of ~ 0.2 ns.

The spatial structure of the laser beam was visualised with a CCD-4M camera in the far field and with a LI-427 vidicon camera in the near field. The automatic diagnostic system we used allowed us to simultaneously measure the energy balance of the laser radiation on the target and the dynamics of foil burn-through with good spatial and temporal resolution and to determine the beam intensity profile on the target surface.

An inhomogeneous 2D plasma may generate spontaneous magnetic fields because of the crossed temperature and density gradients in the target (see, e.g. [18]). The magnetic fields in the region between the critical plasma density surface and evaporation front may also influence the ablation pressure nonuniformity, but conventional optical measurement techniques based on the Faraday rotation of the polarisation plane of a probing laser beam are unsuitable for exploring an overdense plasma. Konash and Lebo [19] analysed the possibility of detecting spontaneous magnetic fields using the scattering of a probing electron

*Attempts were made to simulate such experiments using the Atlant-C Lagrangian code [11], but because of the mesh evolution the computational cost considerably exceeded that with the Euler method.

beam produced by an additional picosecond pulse. The Pico facility includes, in addition to the main (nanosecond) laser, an additional (picosecond) laser, synchronised with the main laser. The picosecond laser generates pulses up to 50 mJ in energy, which offers the possibility of producing a probing electron beam.

4. Experimental results

In the foil burn-through experiments, the intensity profile of the main laser pulse was not deliberately smoothed in order to simulate interference phenomena in multibeam facilities. The speckle pattern on the target surface was recorded by a CCD array camera.

Figures 1–4 present the results of several series of experiments with various spatiotemporal prepulse structures. The data are represented as plots of E_{tr}/E_{in} against E_{in}, where E_{tr} is the energy transmitted through the foil and E_{in} is the laser pulse energy.

In the first series of experiments, the prepulse energy was $E_{pp} = 0.1E_{in}$ and the main-pulse delay relative to the prepulse was $\Delta t = 1.5$ ns. The energy reflected from the foil was 1 %–2 % of E_{in}. The results are presented in Fig. 1. The prepulse is seen to have a significant effect on foil burn-through: it reduces the transmitted energy E_{tr} by about one order of magnitude.

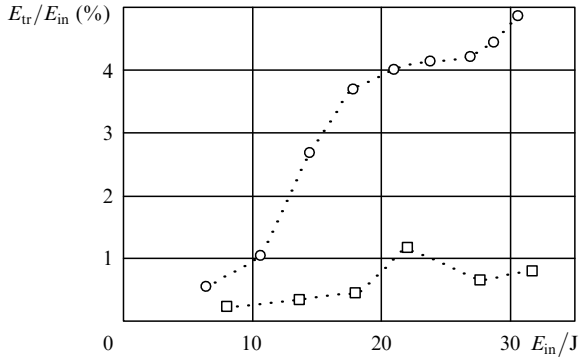

Figure 1. Experimental E_{tr}/E_{in} versus E_{in} data, where E_{tr} is the energy transmitted through the foil and E_{in} is the laser pulse energy: (□) prepulse energy $E_{pp} = 0.1E_{in}$, $\Delta t = 1.5$ ns; (○) no prepulse.

In the second series of experiments, the prepulse energy was substantially lower, $E_{pp} = 0.005E_{in}$, while the delay time was the same, $\Delta t = 1.5$ ns. As a result, the smoothing effect was much weaker (Fig. 2). Similar results were obtained in the third series of experiments, at a high prepulse energy, $E_{pp} = 0.5E_{in}$ (Fig. 3). The smoothing effect in those experiments was stronger than that in the second series but substantially weaker than in the first series. In addition, the reflected energy increased to 4 %–5 % of E_{in}. The likely reason for this is that the prepulse contained speckles with a peak intensity comparable to that of the speckles in the main pulse.

Figure 4 presents the results of the fourth series of experiments, in which the prepulse energy was the same as in the first series, but the main-pulse delay relative to the prepulse was increased by almost a factor of 3, to 4 ns. Under these conditions, the effect of the prepulse was the same as in the second series of experiments, and the reflected energy was ~ 2 % of E_{in}.

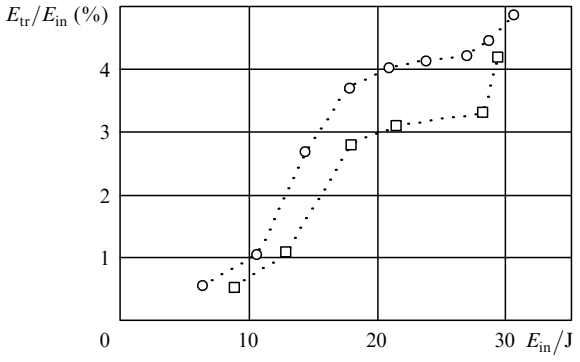

Figure 2. Same as in Fig. 1 with $E_{pp} = 0.005E_{in}$.

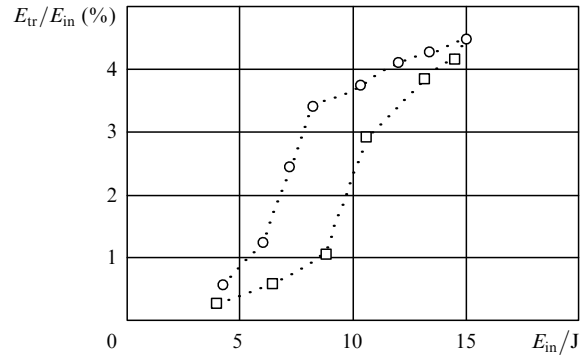

Figure 3. Same as in Fig. 1 with $E_{pp} = 0.5E_{in}$.

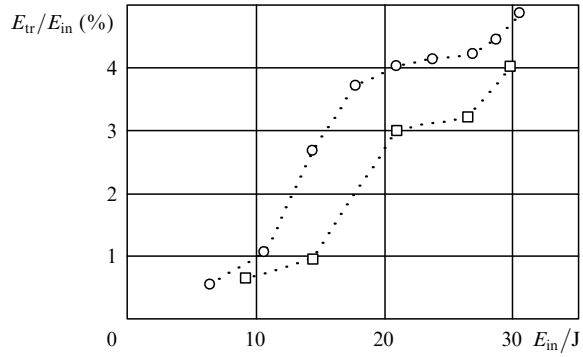

Figure 4. Same as in Fig. 1 with $\Delta t = 4$ ns.

5. Numerical modelling

To gain greater insight into the mechanism underlying the prepulse effect on the smoothing of ablation pressure nonuniformities in the laser-plasma corona, we performed numerical simulations with NUTCY. Using difference methods, we solved a set of hydrodynamic equations for multicomponent media in conjunction with nonlinear 2D heat and radiative transfer equations. (Note that analogous 3D problems incur high computational cost even with modern computing facilities). The governing equations were

$$\frac{\partial \rho}{\partial t} + \frac{1}{r}\frac{\partial (r\rho u)}{\partial r} + \frac{\partial (\rho w)}{\partial z} = 0,$$

$$\frac{\partial (\rho u)}{\partial t} + \frac{1}{r}\frac{\partial (r\rho u^2)}{\partial r} + \frac{\partial (\rho u w)}{\partial z} + \frac{\partial p}{\partial r} = 0,$$

$$\frac{\partial(\rho w)}{\partial t}+\frac{1}{r}\frac{\partial(r\rho uw)}{\partial r}+\frac{\partial(\rho uw)}{\partial z}+\frac{\partial p}{\partial z}=0,$$

$$\frac{\partial e}{\partial t}+\frac{1}{r}\frac{\partial(ru(e+p))}{\partial r}+\frac{\partial((e+p)w)}{\partial z}=-\mathrm{div}\, q_T-\mathrm{div}\, q_\mathrm{L},$$

where

$$e=\rho\left(\varepsilon+\frac{u^2+w^2}{2}\right);\quad p=(\gamma-1)\varepsilon\rho;$$

ρ is the plasma density; γ is the adiabatic exponent; ε is the specific internal energy; p is pressure; $q_T=\varkappa\,\mathrm{grad}\,T$ is the electron component of the heat flux; and q_L is the laser beam intensity. The electron thermal conductivity was taken in the Spitzer–Braginsky form: $\varkappa=\varkappa_0 T^{2.5}$. Computations were performed in Eulerian cylindrical coordinates, r and z, with the plasma flow velocity vector components designated u and w, respectively.

In our simulations, ionisation and recombination processes are left out of account, the charges of the ions, Z_i, are assumed constant, and the equation of state of an ideal gas is used. Re-emission from the plasma is also neglected. The laser beam propagates along the z axis, and inverse bremsstrahlung absorption is taken into account. The laser energy reaching the critical surface is absorbed near it. To solve the hydrodynamic equations, we used second order accurate explicit schemes and special flux limiters [8]. Heat transfer was simulated using implicit difference schemes.

Preliminary simulation results were reported previously [4]. Here, we present a systematic description and detailed analysis of the results. The focal spot radius in our experiments was 30–50 μm, and the radius of an individual speckle was about 5 μm. The number of observed speckles was 20–30, and their intensity was at least an order of magnitude above the average beam intensity. The total speckle area was an order of magnitude smaller than the focal spot area, and the foil thickness ($\sim$ 5 μm) was an order of magnitude smaller than the spot radius. As shown earlier [7], speckles pierce the unevaporated material. A divergent shock wave propagating through the condensed part of the target pulls apart the dense material. Since the distance between speckles is an order of magnitude greater than their radius, and their effects on the plasma are asynchronous, the average density of the condensed material varies only slightly, and the effects of speckles can be considered independent. In view of this, our numerical simulations deal with piercing of a condensed layer by one speckle.

The modelling scheme was as follows: two triangular pulses representing the prepulse and main pulse, separated by time interval Δt, were incident on aluminium metal foil. The pulses had the maximum intensity, I_1 and I_2, respectively, on the target surface at $r=0$. The radial intensity profile of the prepulse was uniform, and that of the main pulse was Gaussian, representing the influence of one speckle. In other words, the transverse I_2 profile was

$$I_2(r,t)=q_1(t)q_2(r),$$

where $q_1(t)$ is the time-dependent incident power; $q_2(r)=C/\exp(r/R_\mathrm{f})^2$;

$$C=\frac{1}{\pi R_\mathrm{f}^2\left\{1-\exp\left[-(R_0/R_\mathrm{f})^2\right]\right\}}$$

is the normalising constant; R_0 is the simulation region radius; and R_f is the effective focal spot radius on the target surface.

In the first series of simulations, the following parameters of the pulses were used: $I_1=2.36\times10^{13}$ W cm^{-2}, $I_2=8.48\times10^{14}$ W cm^{-2} (intensity ratio $m=I_2/I_1\approx36$), prepulse radius $R_0=300$ μm and speckle radius $R_\mathrm{f}=5$ μm. At zero delay, irradiation of the target produces a through hole in the foil (Fig. 5a). Note that, in general, the hole is filled with a hot low-density plasma transparent to the laser radiation, which however does not prevent speckles from penetrating through the condensed substance. Increasing the delay to $\Delta t=0.5-1.5$ ns radically alters the situation, resulting in uniform transverse profiles of the pressure and density (Fig. 5b).

In the second series of simulations, we varied the intensity ratio of the prepulse and main pulse: $m=90-300$ (I_2 was the same as in the first series). The delay time Δt was 0.5 and 1.5 ns. At $\Delta t=0.5$ ns, a uniform ablation pressure was obtained for $m\leqslant200$ (Fig. 6). When the time delay was increased to 1.5 ns, complete smoothing was achieved at $m\leqslant250$. Therefore, in the conditions under consideration and at main-pulse delays relative to the prepulse from 0.5 to 1.5 ns, the prepulse intensity may be one to two orders of magnitude lower than the main pulse intensity. This is important from the viewpoint of the rational use of laser energy.

In the third series of simulations, we examined the smoothing effect in a broader range of delay times ($\Delta t=0-3$ ns) at a constant intensity ratio $m=250$. At $\Delta t=0.5$ ns, partial piercing of the plasma layer occurs, but overdense layers persist on the axis until the end of the pulse (Fig. 7). At $\Delta t=1-1.5$ ns, the smoothing effect of the prepulse is most pronounced. For $\Delta t>1.5$ ns, the effect is weaker.

Thus, we are led to conclude that there is an optimal main-pulse delay relative to the prepulse for speckle suppression, which is 1–1.5 ns under the conditions of this study.

Finally, in the fourth series of simulations we studied the effect of speckle size on the rate of foil burn-through and assessed the feasibility of reducing it using a prepulse. The simulations were performed with $I_2=8.48\times10^{14}$ W cm^{-2} and $m\approx100$. The only variable parameter was the speckle size: $R_\mathrm{f}=5$, 10 and 20 μm. As shown earlier [7], increasing the speckle size impedes speckle penetration through material. However, in the system under consideration, no through hole was formed in the plasma layer during the laser pulse even at $R_\mathrm{f}=5$ μm.

6. Conclusions

The present results indicate that a laser prepulse has a significant effect on the smoothing of ablation pressure nonuniformities in the laser-plasma corona and that it may reduce the effect of hydrodynamic instabilities on the compression of spherical targets. Our experiments show almost an order of magnitude decrease in the fraction of laser energy transmitted through aluminium foil and suggest that there are optimal prepulse energies and main-pulse delays. Mathematical modelling of the processes involved gives further insight into the dynamics of plasma density in relation to the spatiotemporal prepulse structure. The possible effect of spontaneous magnetic fields on the

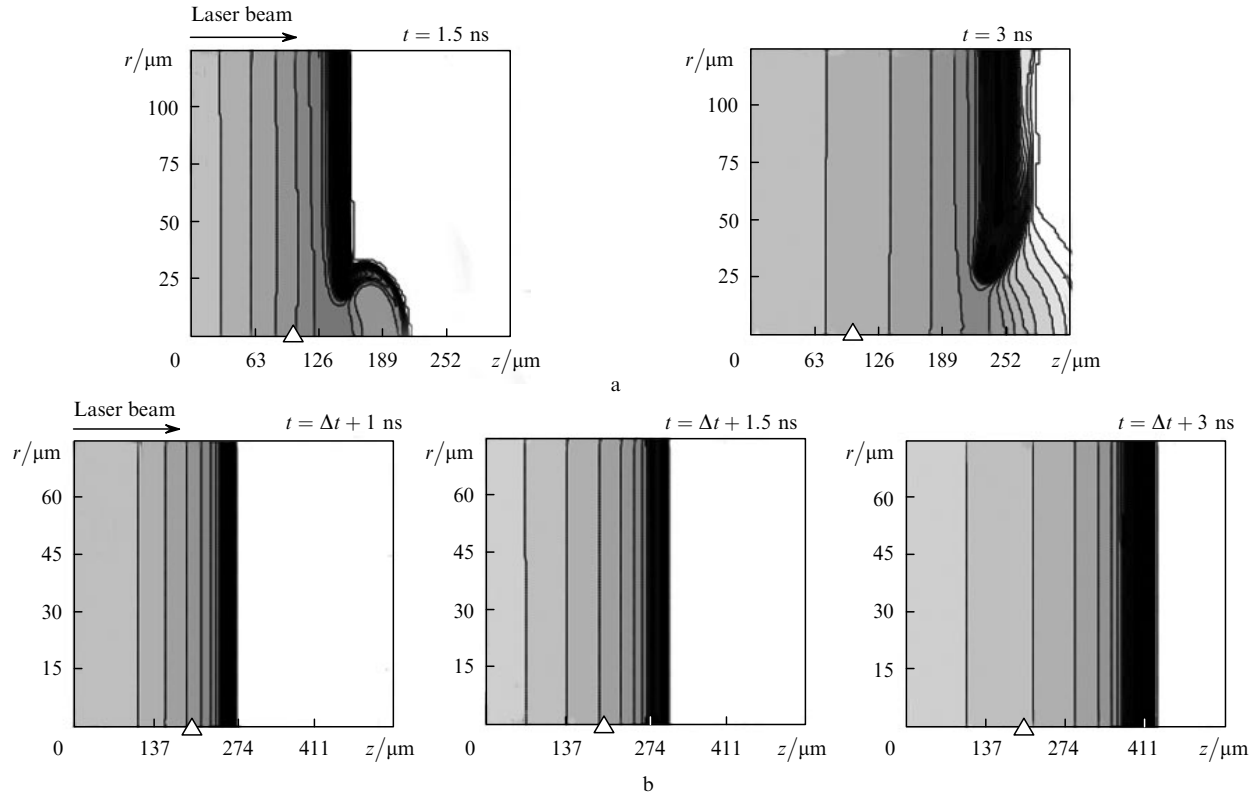

Figure 5. Simulated plasma density near the unevaporated part of the target at times $t = 1.5$ ns (the peak intensity of the heating pulse) and 3 ns (the end of the laser pulse): (a) zero speckle delay relative to the prepulse; (b) the target was exposed to a laser prepulse with the peak intensity $I_1 = 2.358 \times 10^{13}$ W cm^{-2} before the arrival of a speckle with the maximum intensity $I_2 = 8.48 \times 10^{14}$ W cm^{-2} ($\Delta t = 1$ ns). The open triangles indicate the initial position of the target surface, where the laser radiation is absorbed.

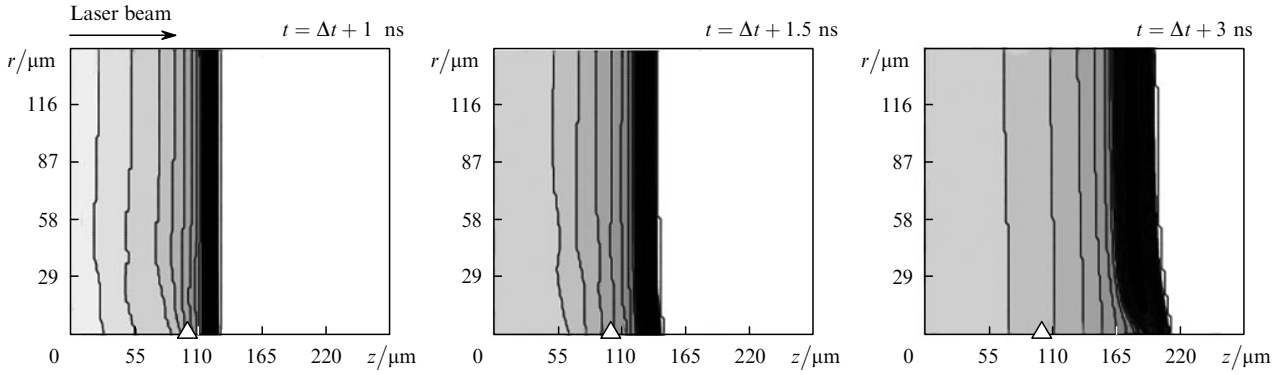

Figure 6. Same as in Fig. 5 with $m = 200$, $\Delta t = 0.5$ ns, $I_1 = 4.24 \times 10^{12}$ W cm^{-2} and $I_2 = 8.48 \times 10^{14}$ W cm^{-2}.

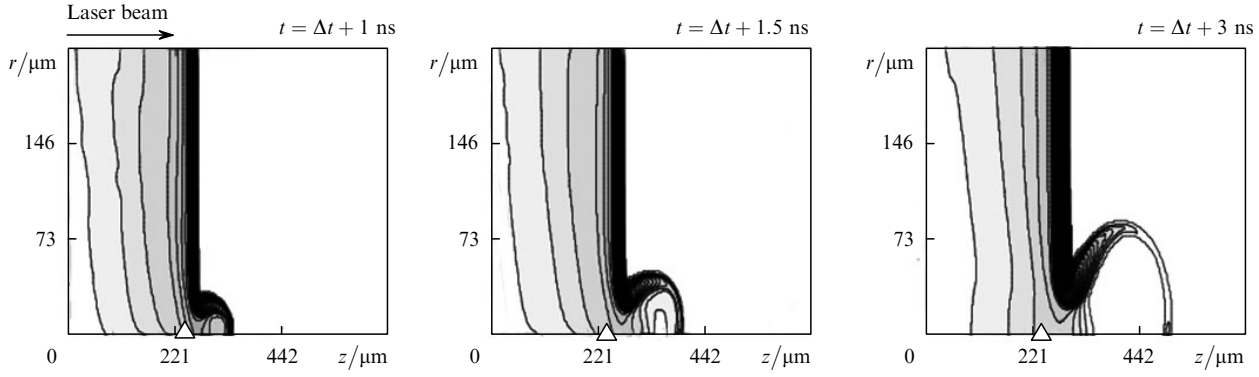

Figure 7. Same as in Fig. 5 with $m = 250$, $\Delta t = 0.5$ ns, $I_1 = 3.4 \times 10^{12}$ W cm^{-2} and $I_2 = 8.48 \times 10^{14}$ W.

processes in the plasma was here left out of account. In future work, a probing electron beam generated by a picosecond pulse will be employed to study overdense plasma regions using electron scattering by spontaneous magnetic fields.

Exposure of the fusion target to a laser prepulse appears to be an effective strategy for smoothing ablation pressure nonuniformities, along with other approaches, relying on optical components and induced spatial incoherence for laser beam smoothing and also on targets with low-density ablators.

Acknowledgements. This work was supported by the Russian Foundation for Basic Research (Grant No. 08-02-00913-a).

References

1. Basov N.G., Mikhailov Yu.A., Sklizkov G.V., et al. *Lazernye termoyadernye ustanovki* (Laser Fusion Plants) (Moscow: VINITI, 1984) p. 25.
2. Basov N.G., Lebo I.G., Rozanov V.B. *Fizika lazernogo termoyadernogo sinteza* (Physics of Laser Fusion) (Moscow: Znanie, 1988).
3. Bokov N.N., Bunatyan A.A., Lykov V.A., et al. *Zh. Prikl. Mekh. Tekh. Fiz.*, **134** (4), 20 (1982).
4. Ilyasov A.O., Lebo I.G., Mikhailov Yu.A., et al. *Kvantovaya Elektron.*, **35** (7), 641 (2005) [*Quantum Electron.*, **35** (7), 641 (2005)].
5. Gamaly E.G., Favorsky A.P., Fedyanin A.O., et al. *Laser Part. Beams*, **8**, 399 (1994).
6. Lebo I.G., Rohlena K., Rozanov V.B., Tishkin V.F. *Kvantovaya Elektron.*, **23**, 71 (1996) [*Quantum Electron.*, **26**, 69 (1996)].
7. Ivanov V.V., Kutsenko A.V., Lebo I.G., et al. *Zh. Eksp. Teor. Fiz.*, **116**, 1287 (1999).
8. Lebo I.G., Tishkin V.F. *Issledovanie gidrodinamicheskoi neustoichivosti v zadachakh lazernogo termoyadernogo sinteza* (Hydrodynamic Instability in Laser Fusion Problems) (Moscow: Fizmatlit, 2006) pp 175 – 178.
9. Iskakov A.B., Tishkin V.F., Lebo I.G., et al. *Phys. Rev. E*, **61**, 842 (2000).
10. Limpouch J., Iskakov A.B., Masek K., et al. *Laser Part. Beams*, **20**, 93 (2002).
11. Iskakov A.B., Lebo I.G., Tishkin V.F. *J. Rus. Laser Res.*, **21** (3), 247 (2000).
12. Lebo I.G., Rozanov V.B., Tishkin V.F. *Kvantovaya Elektron.*, **24** (8), 721 (1997) [*Quantum Electron.*, **27** (8), 702 (1997)].
13. Lebo I.G., Rozanov V.B., Tishkin V.F. *Laser Part. Beams*, **12** (3), 361 (1994).
14. Dunne M., Borghesi M., Ivase A., et al. *Phys. Rev. Lett.*, **75** (21), 3858 (1995).
15. Bugrov A.E., Burdonskii I.N., Gavrilov V.V., et al. *Zh. Eksp. Teor. Fiz.*, **111**, 903 (1997).
16. Gus'kov S.Yu., Rozanov V.B. *Kvantovaya Elektron.*, **24** (8), 715 (1997) [*Quantum Electron.*, **27** (8), 696 (1997)].
17. Rozanov V.B. *Usp. Fiz. Nauk*, **174** (4), 371 (2005).
18. Gamalii E.G., Lebo I.G., Rozanov V.B., Tishkin V.F. *Tr. Fiz. Inst. im. P.N. Lebedeva, Ross. Akad. Nauk*, **149**, 4 (1985).
19. Konash P.V., Lebo I.G. *Kvantovaya Elektron.*, **36** (8), 767 (2006) [*Quantum Electron.*, **36** (8), 767 (2006)].